

# Phase Diagram and Spin Dynamics in Volborthite with a Distorted Kagomé Lattice

M. Yoshida, M. Takigawa, H. Yoshida, Y. Okamoto, and Z. Hiroi  
*Institute for Solid State Physics, University of Tokyo, Kashiwa, Chiba 277-8581, Japan*  
 (Dated: November 6, 2018)

We report  $^{51}\text{V}$ -NMR study on a high-quality powder sample of volborthite  $\text{Cu}_3\text{V}_2\text{O}_7(\text{OH})_2 \cdot 2\text{H}_2\text{O}$ , a spin-1/2 Heisenberg antiferromagnet on a distorted kagomé lattice formed by isosceles triangles. In the magnetic fields below 4.5 T, a sharp peak in the nuclear spin-lattice relaxation rate  $1/T_1$  accompanied with line broadening revealed a magnetic transition near 1 K. The low temperature phase shows anomalies such as a Lorentzian line shape, a  $1/T_1 \propto T$  behavior indicating dense low energy excitations, and a large spin-echo decay rate  $1/T_2$  pointing to unusually slow fluctuations. Another magnetic phase appears above 4.5 T with less anomalous spectral shape and dynamics.

PACS numbers: 75.30.Kz, 76.60.-k, 75.40.Gb

The search for exotic ground states in two-dimensional (2D) spin systems with frustrated interactions has been a challenge in condensed matter physics [1]. In particular, the ground state of the spin-1/2 Heisenberg model with a nearest neighbor interaction on a kagomé lattice, a 2D network of corner-sharing equilateral triangles, is believed to show no long-range magnetic order. Theories have proposed various ground states such as spin liquids with no broken symmetry with [2] or without [3] a spin-gap or symmetry breaking valence-bond-crystal states [4]. Candidate materials known to date, however, depart from the ideal kagomé model in one way or another such as disorder, structural distortion, anisotropy, or longer range interactions. Volborthite  $\text{Cu}_3\text{V}_2\text{O}_7(\text{OH})_2 \cdot 2\text{H}_2\text{O}$  is an example, which has distorted kagomé layers formed by isosceles triangles. Consequently, it has two Cu sites and two kinds of exchange interactions as shown in the inset of Fig. 1. The magnetic susceptibility  $\chi$  obeys the Curie-Weiss law  $\chi = C/(T + \theta_W)$  above 200 K with  $\theta_W = 115$  K, exhibits a broad maximum at 20 K, and approaches a finite value at the lowest temperatures, indicating absence of a spin gap. The specific heat and  $\chi$  data revealed no magnetic order down to 2 K, much lower than  $\theta_W$  [5]. This indicates strong effects of frustration common to the geometry of the kagomé lattice, even though the difference between  $J$  and  $J'$  should partially lift the massive degeneracy of low energy states of the ideal kagomé model.

Dynamic measurements, however, suggest a magnetic transition at a lower temperature. The nuclear spin-lattice relaxation rate  $1/T_1$  at the V sites shows a peak at 1.4 K, below which the nuclear magnetic resonance (NMR) spectrum begins to broaden [6]. The muon spin relaxation ( $\mu\text{SR}$ ) experiments also detected slowing down of spin fluctuations with decreasing temperature towards 1 K [7]. These dynamic anomalies coincide with the appearance of hysteresis in  $\chi$ , i.e. the difference between field-cooled and zero-field-cooled magnetization, suggesting a spin-glass like state [6]. However, impurity effects corresponding to the Curie term in  $\chi$  of more than 0.5 %/Cu of spin-1/2 [5, 8] have been impeding proper

understanding of intrinsic properties of volborthite.

Recently, H. Yoshida *et al.* have succeeded in reducing impurities down to 0.07 % by hydrothermal annealing [9]. Although a small hysteresis of  $\chi$  is still observed below 1 K at 0.1 T, it is rapidly suppressed by magnetic fields of less than 2 T (the dotted line in Fig. 1). They also reported unusual sequential magnetization steps at 4.3, 25.5, and 46 T. In this Letter, we report on the  $^{51}\text{V}$ -NMR experiments using a high-quality powder sample prepared by the same method. We observed a sharp peak of  $1/T_1$  at 0.9 K accompanied by a broadening of the NMR spectrum in the field range 1 – 4.5 T, indicating a magnetic transition unrelated to the hysteresis of  $\chi$ . The results of nuclear relaxation rates, however, revealed

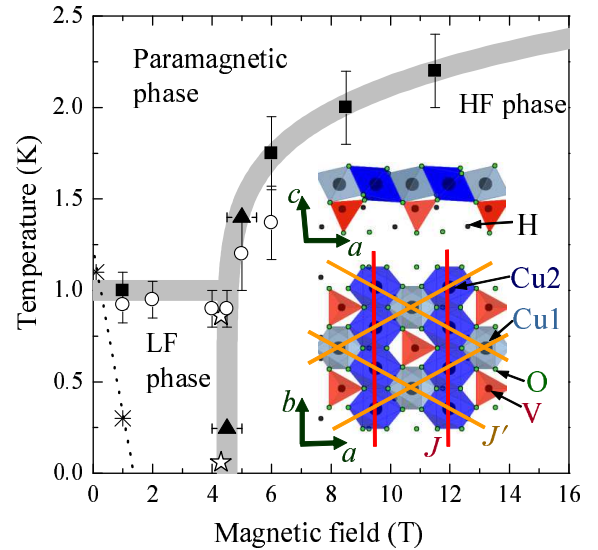


FIG. 1: (color online) Inset: the crystal structure of volborthite. Main panel: the proposed phase diagram. The squares (triangles) represent the phase boundaries determined from the broadening of NMR spectra as a function of temperature (magnetic field). The circles and asterisks indicate the peak of  $1/T_1$  and the onset of hysteresis in  $\chi$ , respectively. The stars indicate the first magnetization step [9]. The lines are guide to the eyes.

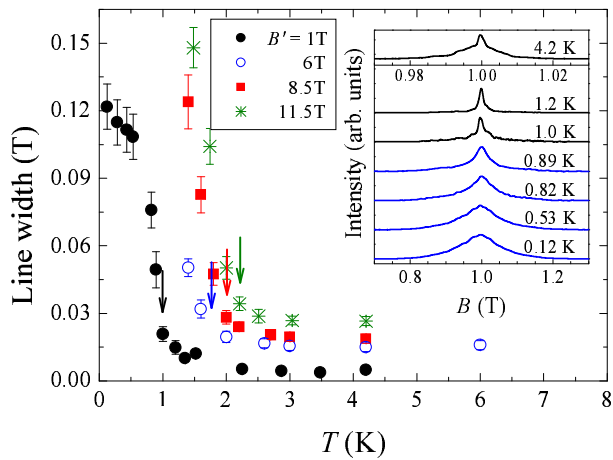


FIG. 2: (color online)  $T$ -dependence of the line width (FWHM) at various magnetic fields. ( $B'$  stands for the center of gravity of the spectrum.) The inset shows the NMR spectra at  $\nu = 11.243$  MHz ( $B' = 1$  T). The horizontal scale is expanded for the data at 4.2 K.

a large weight of low-energy excitations and persistence of anomalously slow spin fluctuations down to  $T = 0$ . We also found another magnetic phase above 4.5 T with distinct spin structure and dynamics. The transition occurs at the same field as the first magnetization step [9].

The NMR spectra were obtained by summing the Fourier transform of the spin-echo signal obtained by the pulse sequence  $\pi/2 - \tau - \pi/2$  at equally spaced magnetic fields  $B$  with a fixed resonance frequency  $\nu$ . Typically  $\tau = 12 - 20$   $\mu\text{s}$  and the pulse width was 1.0–1.8  $\mu\text{s}$ . We determined  $1/T_1$  by fitting the spin-echo intensity  $M(t)$  as a function of the time  $t$  after several saturating comb pulses to the exponential recovery function  $M(t) = M_{eq} - M_0 \exp(-t/T_1)$ , where  $M_{eq}$  is the intensity at thermal equilibrium. When this function did not fit the data due to inhomogeneous distribution of  $1/T_1$ , we used the stretched exponential function  $M(t) = M_{eq} - M_0 \exp\{-(t/T_1)^\beta\}$  to determine the representative value of  $1/T_1$ .

The inset of Fig. 2 shows the  $T$ -dependence of the  $^{51}\text{V}$  NMR spectrum below 4.2 K at  $\nu = 11.243$  MHz corresponding to  $B \sim 1$  T. The spectrum at 4.2 K consists of a sharp central line with the full width at half maximum (FWHM) of  $4 \times 10^{-3}$  T and quadrupole satellite lines (FWHM =  $2 \times 10^{-2}$  T). At high temperatures above 140 K, the magnetic hyperfine shift  $K$  and  $\chi$  follow the same  $T$ -dependence, yielding the hyperfine coupling constant  $A_{hf} = 0.77$  T/ $\mu_B$  consistent with the previous reports [5, 6]. The FWHM of the central line is about a half of the shift, indicating that the hyperfine coupling is dominantly isotropic, which should be attributed to the neighboring six  $\text{Cu}^{2+}$  spins. Below 4.2 K, gradual broadening of the central line smears out the quadrupole structure. In the temperature range 2 – 4 K, the width

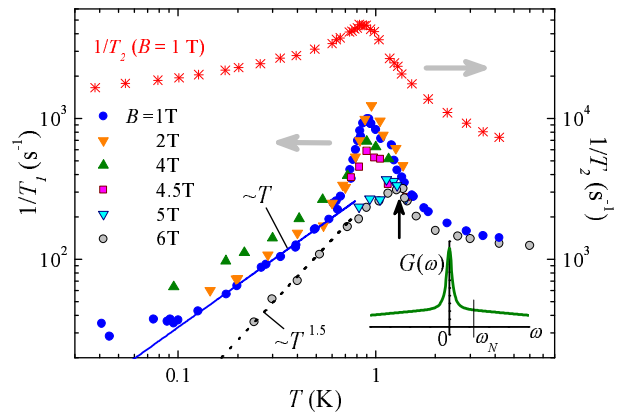


FIG. 3: (color online)  $T$ -dependence of  $1/T_1$  at various magnetic fields  $B$ . The asterisks represent the  $T$ -dependence of  $1/T_2$  at 1 T. The solid (dotted) line shows the power law dependence  $T^\alpha$  with  $\alpha = 1$  (1.5). The inset shows a schematic illustration of  $G(\omega)$  with two distinct frequency scales.

of the whole spectrum is about a factor four smaller than the previous results [5, 6], indicating much less disorder in our sample.

The spectrum shows a sudden broadening below 1 K and the width tends to saturate below 0.5 K, where the line shape is approximately Lorentzian. The  $T$ -dependence of the line width (FWHM of the whole spectrum) is shown in Fig. 2. Since the width at low temperatures is independent of  $B$  below 3.5 T as will be shown later (Fig. 4), the symmetric line broadening must be due to spontaneous staggered moments, which remain finite at zero field. However, the line shape does not look like that of an ordinary antiferromagnet. For a powder sample of an antiferromagnet with a homogeneous magnitude of moments, random orientation of the internal field with respect to the external field yields a rectangular spectral shape. The Lorentzian line shape in volborthite indicates large distribution of the magnitude of moments, suggesting a spin-density-wave like modulation or a lack of long range spatial order. Note that the transition near 1 K is *not* a spin-glass transition reported in the earlier work [6], since the hysteresis in  $\chi$  in our sample is barely visible only below 0.3 K at  $B = 1$  T (Fig. 1 [9]).

Figure 3 shows the  $T$ -dependence of  $1/T_1$  measured at the peak of the spectra for various values of  $B$ . One can recognize an apparent change of behavior near  $B = 4.5$  T. We first discuss the results below 4.5 T. We were able to fit  $M(t)$  to the single exponential function above 1.2 K. Below 1.2 K, however, distribution in  $1/T_1$  let us use the stretched exponential function. The stretch exponent  $\beta$  decreased monotonically with decreasing  $T$  and stayed constant at  $\beta = 0.6$  below 0.8 K down to 40 mK. A sharp peak of  $1/T_1$  is observed at 0.9 K for  $B = 1$  T, which agrees with the onset of line broadening, providing further evidence for a magnetic transition. The transition temperature of 1 K is not far from that

reported by Bert *et al.* (1.4 K) [6]. However, our data show a much sharper peak and the peak value of  $1/T_1$  is nearly an order of magnitude larger than their value. Thus the transition becomes more pronounced when disorder is reduced. The peak temperature of  $1/T_1$  is nearly independent of  $B$  below 4.5 T. This behavior is again in contradiction to the hysteresis in  $\chi$  or the spin-glass-like behavior.

At low temperatures below 0.6 K,  $1/T_1$  varies proportionally to  $T$ . While the magnetic field enhances  $1/T_1$  slightly, the  $T$ -linear behavior is robust up to 4 T. Below 0.1 K,  $1/T_1$  becomes independent of  $T$ , which is most likely caused by impurities. The  $T$ -linear behavior is in strong contrast to what is observed in ordinary antiferromagnets, where nuclear relaxation is caused by the scattering of spin waves. Usually the two-magnon Raman process is dominant for anisotropic hyperfine coupling, while three-magnon process has to be invoked for isotropic coupling [10, 11, 12]. For  $T \gg \Delta$ , where  $\Delta$  is the gap in the spin wave spectrum,  $1/T_1 \propto T^D$  [10, 13] for the two-magnon process, where  $D$  ( $= 3$  or  $2$ ) is the dimensionality of the spin-wave dispersion. The three magnon process also leads to power laws with even larger exponents. In both dimensions,  $1/T_1$  decreases exponentially for  $T \ll \Delta$ . The  $T$ -linear behavior without any sign of a spin gap in volborthite, therefore, indicates anomalously dense low energy excitations at low temperatures.

A possible mechanism for the  $T$ -linear behavior of  $1/T_1$  is the particle-hole excitations in a fermionic system as in metals. Since fermionic elementary excitations (spinons) are proposed for the kagomé systems [3, 14], it is appropriate to compare our data with the value for free fermions given by the Korringa relation,  $1/(T_1TK^2) = 4\pi k_B \hbar (\gamma_N/g\mu_B)^2$ . From the value of the shift at 4.2 K ( $K = 0.40\%$ ), we found that the free fermion value  $1/(T_1T) = 4 \text{ sec}^{-1}\text{K}^{-1}$  is two orders of magnitude smaller than the experimental value  $330 \text{ sec}^{-1}\text{K}^{-1}$ . (Note that  $\chi$  at 1 T is nearly independent of  $T$  below 4 K [9].) Thus the dynamics involves much slower fluctuations than static energy scale set by  $\chi$  or the spinon band width. Another possible origin is the localized zero-energy mode with nearly flat dispersion, as was observed in classical Kagomé systems [15].

Quite surprisingly, even slower fluctuations were revealed from the spin-echo decay rate  $1/T_2$ . Figure 3 also shows the  $T$ -dependence of  $1/T_2$  measured at  $B = 1$  T. The spin-echo intensity exhibits exponential  $\tau$  dependence,  $M(2\tau) \propto \exp(-2\tau/T_2)$ . This means that the fluctuations of the local-field  $h(t)$  causing the spin-echo decay are in the narrowing limit,  $\gamma\sqrt{\langle h^2(t) \rangle}\tau_c \ll 1$ , where  $\tau_c$  is the correlation time. Above 0.9 K,  $1/T_2$  and  $1/T_1$  show similar  $T$ -dependence but largely different values  $r = (1/T_2)/(1/T_1) \sim 50$ . Below 0.9 K, they show qualitatively different behavior.  $1/T_2$  decreases much more slowly than  $1/T_1$  and approaches a large value towards  $T = 0$  ( $r \sim 500$ ).

In general,  $1/T_2$  is the sum of electronic and nuclear contributions,  $1/T_2 = (1/T_2)_e + (1/T_2)_n$ . The first term further consists of two terms due to fluctuations of the hyperfine field perpendicular and parallel to the external field,  $(1/T_2)_e = (1/T_2)_{e\perp} + (1/T_2)_{e\parallel}$ , where  $(1/T_2)_{e\perp} = 1/(2T_1) = (\gamma^2/2) \int_{-\infty}^{\infty} \langle h_{\perp}(0)h_{\perp}(t) \rangle \exp(2\pi i\nu t) dt$  is given by the fluctuation amplitude of  $h_{\perp}(t)$  at the NMR frequency  $\nu$  [16]. On the other hand,  $(1/T_2)_{e\parallel}$  is determined by the longitudinal fluctuations averaged over the time scale of  $T_2$  itself [17, 18], i.e. sensitive to much slower fluctuations in the range of 1–10 kHz.

The large value of  $r$  requires either  $(1/T_2)_n \gg (1/T_2)_e$  or  $(1/T_2)_{e\parallel} \gg (1/T_2)_{e\perp}$ . The former case is excluded for several reasons. First,  $1/T_2$  due to the nuclear dipolar coupling is orders of magnitude smaller than the observed values. Second, we found that  $1/T_2$  at 0.25 K did not depend on the strength of the rf-field in spite of the large line width, proving that like-spin ( $^{51}\text{V}$  nuclei) contribution is negligible. If unlike-spins,  $^{65,63}\text{Cu}$  or  $^1\text{H}$ , have strong indirect coupling to  $^{51}\text{V}$  nuclei,  $\tau_c$  is nothing but  $T_1$  of these unlike spins. Since  $1/T_2$  is proportional to  $\tau_c$  in the narrowing limit, similar  $T$ -dependence of  $1/T_2$  and  $1/T_1$  of  $^{51}\text{V}$  would imply that  $^{63,65}\text{Cu}$  (or  $^1\text{H}$ ) and  $^{51}\text{V}$  have completely opposite  $T$ -dependence of  $1/T_1$ . This sounds extremely unlikely.

Therefore,  $(1/T_2)_{e\parallel} \gg (1/T_2)_{e\perp} = 1/(2T_1)$ . Since only 1 T of field should not be sufficient to induce strong anisotropy in a powder sample, we conclude that  $(1/T_2)_{e\parallel}$  is dominated by spin fluctuations with an extremely small frequency scale, much smaller than the NMR frequency ( $\sim 10$  MHz) but still large enough ( $\geq 10$  kHz) to make  $1/T_2$  of the order of  $10^{-4} \text{ sec}^{-1}$  in the narrowing limit. This implies that the spectral density  $G(\omega) = \int_{-\infty}^{\infty} \langle h(0)h(t) \rangle \exp(i\omega t) dt$  has at least two frequency scales as illustrated in the inset of Fig. 3. One gives the narrow zero-frequency peak that determines  $1/T_2$  and another one characterizes the broad spectrum that determines  $1/T_1$ .

Now we discuss the  $1/T_1$  data above  $B = 4.5$  T (Fig. 3). We fit the data of  $M(t)$  by the single (stretched) exponential function above (below) 1.6 K. The value of  $\beta$  decreased from 0.8 at 1.5 K to 0.25 at 0.14 K. While the sharp peak at 0.9 K observed below 4.5 T is absent, a broader peak appears near 1.3 K (see the arrow in Fig. 3). At low temperatures,  $1/T_1$  at 6 T decreases more rapidly with decreasing temperature, approximately as  $T^{1.5}$ , compared with the data below 4.5 T.

A significant change in the line shape is also observed near 4.5 T. Figure 4(a) shows the  $B$ -dependence of the NMR spectrum at 0.28 K. Below 3.5 T, the spectrum is approximately a Lorentzian with a  $B$ -independent width. At 4 T, two shoulders develop on both sides of the spectrum as indicated by the arrows, which eventually grow as the edges of a rectangular spectrum above 5 T. The results of  $1/T_1$  and the line shape combined together provide convincing evidence for a field-induced transition

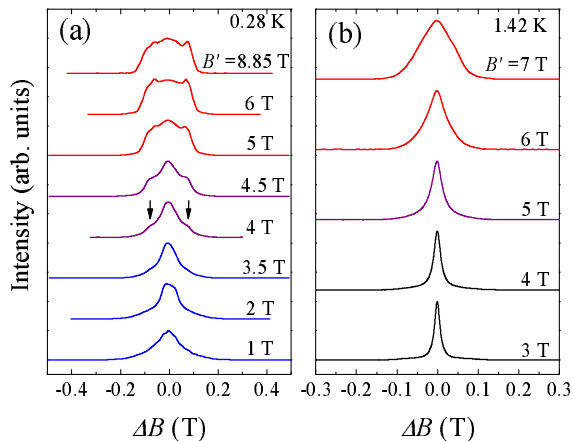


FIG. 4: (color online) Variation of the NMR spectrum with magnetic field at (a)  $T = 0.28$  K and (b)  $1.42$  K. The horizontal axis represents the shift due to antiferromagnetic moments:  $\Delta B = B - \nu/\gamma(1+K)$ , where  $\gamma$  and  $K$  is the gyromagnetic ratio of  $^{51}\text{V}$  (11.1988 MHz/T) and the magnetic hyperfine shift at  $4.2$  K (0.4 %), respectively.

near  $4.5$  T. The rectangular spectral shape in the high field phase is compatible with homogeneous magnitude of moments. We emphasize that  $4.5$  T is close to the field at which the first magnetization step was observed [9].

In order to determine the phase diagram, we plot  $T$ -dependence of the line width at several fields in addition to the data at  $1$  T in Fig. 2. The onset of line broadening indicated by the arrows shifts to higher temperatures with increasing field. Figure 1 shows the  $T$ - $B$  phase diagram thus determined (solid squares). The peak temperatures of  $1/T_1$  are also displayed by the open circles. Three phases can be identified: the paramagnetic (P), low field (LF), and high field (HF) phases. It is remarkable that the transition temperature from P to LF phases is independent of  $B$  up to  $4$  T. Note that there is no anomaly in the  $T$ -dependence of  $\chi$  at  $1$  T [9]. However, recent precise measurements of heat capacity revealed a weak anomaly near  $1$  K [19] not detected before. In contrast, the transition between the P and HF phases moves to higher temperatures with increasing field. To further confirm the boundary between the P and HF phases, we examined the  $B$ -dependence of the spectrum at  $1.4$  K (Fig. 4b). The line width varies linearly with  $B$  below  $4$  T, consistent with the paramagnetic behavior. However, it shows a sudden large increase above  $5$  T, supporting the transition directly from the P to HF phases. The transitions determined from the  $B$ -dependence of the spectra are shown by the triangles in Fig. 1. The HF phase appears less anomalous than the LF phase since the line shape is compatible with the ordinary antiferromagnets and the power law behavior of  $1/T_1$  is closer to the prediction of the spin wave theory in 2D.

In conclusion, we found two magnetic phases in volborthite. The low field phase is anomalous in various aspects: a large variation in the magnitude of moments, dense low frequency excitations characterized by two distinct frequency scales, one of which is extremely small, and the transition insensitive to magnetic field. The high field phase appears less anomalous. Possible magnetic order has been discussed for distorted kagomé systems for the case of either  $J/J' > 1$  [20] or  $J/J' < 1$  [21]. Magnetic order in undistorted kagomé systems can be induced by the Dzyaloshinskii-Moriya interaction [22] or longer range interactions [23]. What causes the magnetic transition in volborthite remains an open issue.

We thank H. Tsunetsugu and F. Mila for stimulating discussions and Y. Nakazawa for disclosing unpublished data. The work was supported by the G-COE program and by Grant-in-Aids for Scientific Research on Priority Areas "Novel States of Matter Induced by Frustration" (19052003) from MEXT Japan.

- 
- [1] G. Misguich and C. Lhuillier, in *Frustrated Spin Systems*, edited by H. T. Diep (World-Scientific, Singapore, 2005), p. 229.
  - [2] C. Waldtmann *et al.*, *Eur. Phys. J. B* **2**, 501 (1998).
  - [3] M. Hermele *et al.*, *Phys. Rev. B* **77**, 224413 (2008).
  - [4] R. R. P. Singh and D. A. Huse, *Phys. Rev. B* **76**, 180407(R) (2007).
  - [5] Z. Hiroi *et al.*, *J. Phys. Soc. Jpn.* **70**, 3377 (2001).
  - [6] F. Bert *et al.*, *Phys. Rev. Lett.* **95**, 087203 (2005).
  - [7] A. Fukaya *et al.*, *Phys. Rev. Lett.* **91**, 207603 (2003).
  - [8] F. Bert *et al.*, *J. Phys. Condens. Matter.* **16**, S829 (2004).
  - [9] H. Yoshida *et al.*, *J. Phys. Soc. Jpn.* **78**, 043704 (2009).
  - [10] T. Moriya, *Prog. Theor. Phys.* **16**, 23 (1956).
  - [11] T. Moriya, *Prog. Theor. Phys.* **16**, 641 (1956).
  - [12] D. Beeman and P. Pincus, *Phys. Rev.* **166**, 359 (1968).
  - [13] F. Mila and T. M. Rice, *Phys. Rev. B* **40**, 11382 (1989).
  - [14] Z. Hao and O. Tchernyshyov, arXiv:0902.0378v2.
  - [15] K. Matan *et al.*, *Phys. Rev. Lett.* **96**, 247201 (2006).
  - [16] Since the quadrupole splitting is small, the enhancement of  $1/T_2$  for selective excitation of a quadrupole split line (R. E. Walsteadt, *Phys. Rev. Lett.* **19**, 146 (1967)) is not relevant in our case.
  - [17] C. H. Recchia, K. Gorny, and C. H. Pennington, *Phys. Rev. B* **54**, 4207 (1996).
  - [18] The spin-echo decay due to fluctuations of  $h_{\parallel}(t)$  is expressed as  $M(2\tau)/M(0) = \langle \cos \left[ \gamma \left( \int_0^{\tau} h_{\parallel}(t) dt - \int_{\tau}^{2\tau} h_{\parallel}(t) dt \right) \right] \rangle$ . By assuming a Gaussian distribution for the accumulated phase, the argument of the cosine function, one obtains an exponential spin-echo decay in the narrowing limit [17].
  - [19] S. Yamashita and Y. Nakazawa, unpublished.
  - [20] A. P. Schnyder, O. A. Starykh, and L. Balents, *Phys. Rev. B* **78**, 174420 (2008).
  - [21] F. Wang, A. Vishwanath, and Y. B. Kim, *Phys. Rev. B* **76**, 094421 (2007).
  - [22] O. Cépas *et al.*, *Phys. Rev. B* **78**, 140405(R) (2008).
  - [23] J.-C. Domenge *et al.*, *Phys. Rev. B* **72**, 024433 (2005).